NANO LETTERS

LETTER

pubs.acs.org/NanoLett

Localized Temperature and Chemical Reaction Control in Nanoscale Space by Nanowire Array

C. Yan Jin,[†] Zhiyong Li,[‡] R. Stanley Williams,[§] K.-Cheol Lee,[∥] and Inkyu Park*[,†]

[†]Department of Mechanical Engineering and KI for the NanoCentury, Korea Advanced Institute of Science and Technology (KAIST), Daejeon, Republic of Korea

[‡]Intelligent Infrastructure Lab and [§]NanoElectronics Research Group, Hewlett-Packard (HP) Laboratory, Palo Alto, California 94304-1126, United States

[∥]Division of Physical Metrology, Korea Research Institute of Standard and Science (KRISS), Daejeon, Republic of Korea

ABSTRACT: We introduce a novel method for chemical reaction control with nanoscale spatial resolution based on localized heating by using a well-aligned nanowire array. Numerical and experimental analysis shows that each individual nanowire could be selectively and rapidly Joule heated for local and ultrafast temperature modulation in nanoscale space (e.g., maximum temperature gradient 2.2 K/nm at the nanowire edge; heating/cooling time < 2 μs). By taking advantage of this capability, several nanoscale chemical reactions such as polymer decomposition/cross-linking and direct and localized hydrothermal synthesis of metal oxide nanowires were demonstrated.

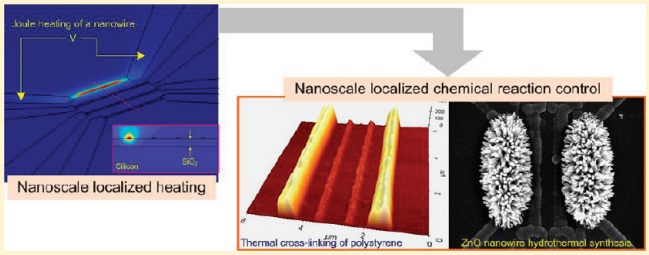

KEYWORDS: Nanowire array, local heating, nanoscale chemical reaction, polymer decomposition, polymer cross-linking, metal oxide nanowire

Recently, there have been great interest and active research on small-scale localized heating, especially in temperature-mediated biology and chemistry. Individually controllable microheater array devices have been developed for local temperature control without crosstalk between each heater[1−3] in microscale space. By use of these microheater array devices, programmed manipulation of proteins[1] and target-specific biological treatment such as cell lysis[2] and protein synthesis[3] have been demonstrated. These devices provide novel platforms for studying local biological and chemical phenomena. Furthermore, study of chemical kinetics or control of a fast chemical reaction is potentially possible due to the small heat capacity of microheaters. Microheaters have also been used for the selective synthesis of nanomaterials and their facile integration on the functional electronic devices such as sensors[4] and optoelectronic components.[5]

Recently, efforts on temperature localization went further from microscale to nanoscale spatial resolution. With the local temperature controllability at the nanoscale, cancer cell lysis without attacking surrounding normal cells was achieved.[6] Also, nanoscale heating was used to generate nanopatterns for ultra-high-density optical information recording[7,8] and light-emitting diodes (LEDs) with improved light extraction efficiency.[9] In addition, ultrafast switching of the phase-change materials between amorphous or crystalline states for a high-speed memory storage device was achieved through nanoscale localized heating.[10,11,26] Other researchers have studied the Joule heating of a single metal nanowire during the fabrication of nanogaps for single molecule electronic devices through enhanced electromigration at elevated temperatures.[12] Furthermore, in sensor applications, it was found that the response and recovery time of nanowire-based gas sensors could be improved by self-heating of the nanowires.[13,14] Although various novel applications of nanoscale temperature control have been demonstrated, either expensive laser systems[6−9] or laborious assembly processes of individual nanowires (nanotubes)[10,11,26] were required. Furthermore, in the case of nanowire (nanotube) heaters,[10−12] spatial controllability of the local temperature field was limited since only a single nanowire was used instead of highly aligned arrays of multiple nanowires (nanotubes).

In this Letter, we introduce a well-aligned nanowire array fabricated by a top-down nanofabrication process,[15−18] which allows electrical addressing of individual nanowires for selective and localized heating with nanoscale spatial resolution and its applicability for nanoscale chemical reaction control. Figure 1 shows the working principle of localized heating and selective chemical reaction control in nanoscale space by utilizing the nanowire Joule heaters. When an electrical bias is applied across the nanowire, highly localized Joule heating along the nanowire results in local temperature increase in the close vicinity of the heated nanowire. Consequently, thermally activated chemical reactions (i.e., endothermic reactions) are induced only around the heated nanowires.

Figure 2a shows a schematic diagram of the nanowire heater array device. Material selection and geometry design for each component of the device are important factors for heat localization. Chrome (Cr) and chrome/gold (Cr/Au) were chosen as the materials for nanowire and electrical interconnection,

Received: August 2, 2011
Revised: September 19, 2011
Published: October 03, 2011

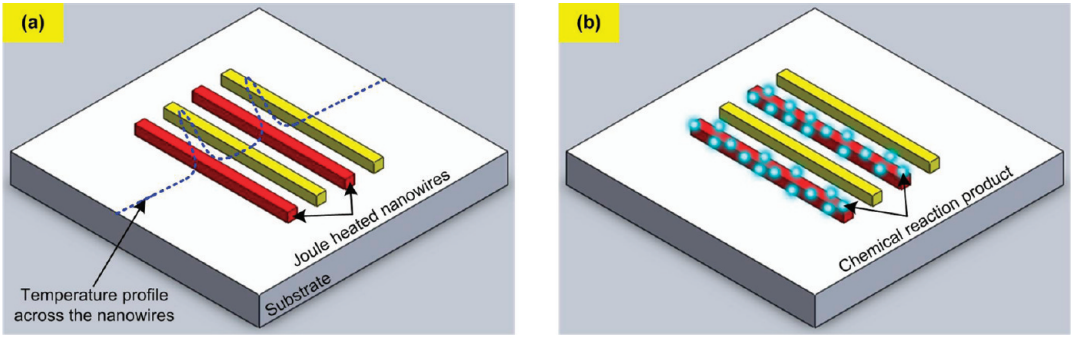

Figure 1. Working principle of nanoscale local chemical reaction control by using an individually addressable nanowire heater array: (a) temperature profile across the nanowires when nanowires #1 and #3 (from left) are Joule-heated and (b) chemical reaction occurring only along the Joule-heated nanowires.

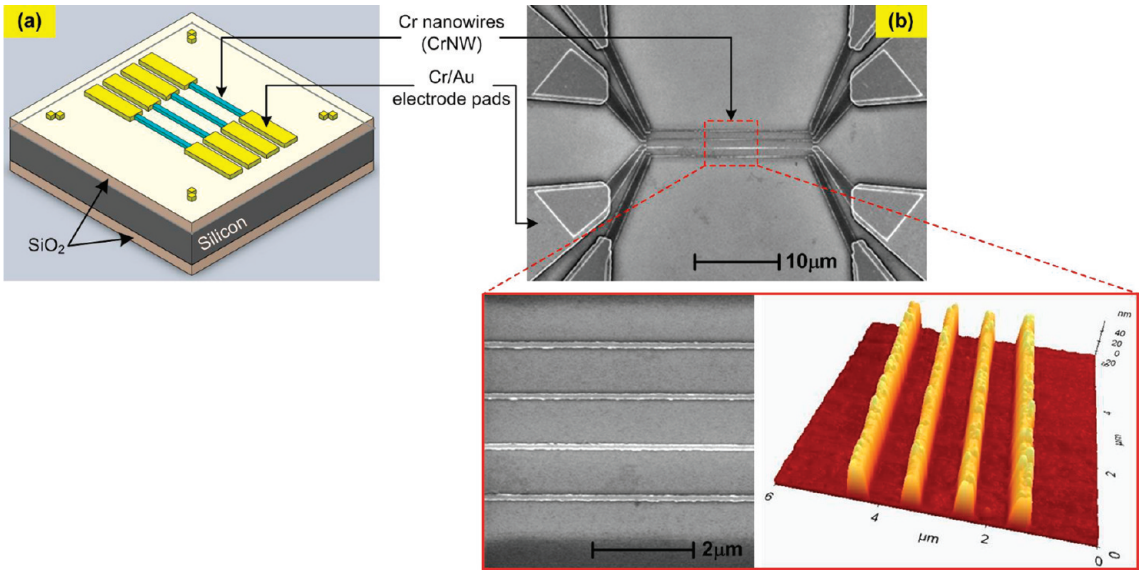

Figure 2. Nanowire heater array device: (a) design schematic and (b) SEM/AFM images of the fabricated device.

respectively. Since the electrical resistivity of Cr is ~6 times bigger (at room temperature, for bulk phase) than that of Au and the aspect ratio (length to width) of nanowires is much larger than other interconnection parts in the circuit, most of the voltage drop and power consumption occur across the nanowires when electrical bias is applied. Power consumption concentrated in extremely small volume of nanowire (ex. thermal power consumption of 1.89×10^{17} J/m^3 at an electrical bias of 1 V) results in highly localized and selective heating in nanoscale space. The Cr nanowires and electrical interconnection circuit were fabricated on Si/SiO_2 substrate by a top-down fabrication method (e-beam/UV lithography, e-beam evaporation of metal layer, and lift-off processes). The scanning electron microscopy (SEM) and atomic force microscopy (AFM) images of the fabricated Cr nanowire array with line width of ~110 nm are shown in Figure 2b.

Temperature distribution of the nanowire-array-based heater was numerically analyzed by COMSOL Multiphysics software and then experimentally verified by scanning thermal microscopy (SThM). For the numerical analysis, a three-dimensional model was used as shown in Figure 3a. An array of four Cr nanowires (width = 100 nm, length = 4 μm (nanowire #1 and #4 from left) and 5 μm (nanowire #2 and #3), thickness = 50 nm, and pitch = 1 μm) is located on a SiO_2 thin film (area = 60 μm × 60 μm) that is thermally grown on a p-type Si wafer (area = 60 μm × 60 μm; thickness = 500 μm). In order to investigate the thickness effect of a thermal insulation layer (SiO_2) on the heat localization, the analysis was performed for two different thicknesses of SiO_2 layers (t_{SiO_2} = 0.33 and 2 μm). The electrical conductivities for Cr, Au, SiO_2, and Si are 7.54×10^{-5}, 4.42×10^{-6}, 0, and 10 S/m, respectively. The thermal conductivities for Cr, Au, SiO_2, and Si are 93.7, 317, 1.4, and 163 W/(m·K), respectively. Heat generated by Cr nanowire is dissipated by thermal conduction to Si/SiO_2 substrate and Cr/Au interconnections and by thermal convection to surrounding environment (stationary air at atmospheric pressure). Since all boundaries are far away from the nanowire array and heat generated by the nanowires is very small, the temperature of all the boundaries was fixed at 293.15 K. From the simulation results in Figure 3b, it is observed that a highly localized temperature distribution is created by Joule heating of individual nanowires. For example, the maximum temperature at the center of nanowire is raised up to 744.4 K while it drops down to 442.9 K at a distance of 200 nm from the center of heated

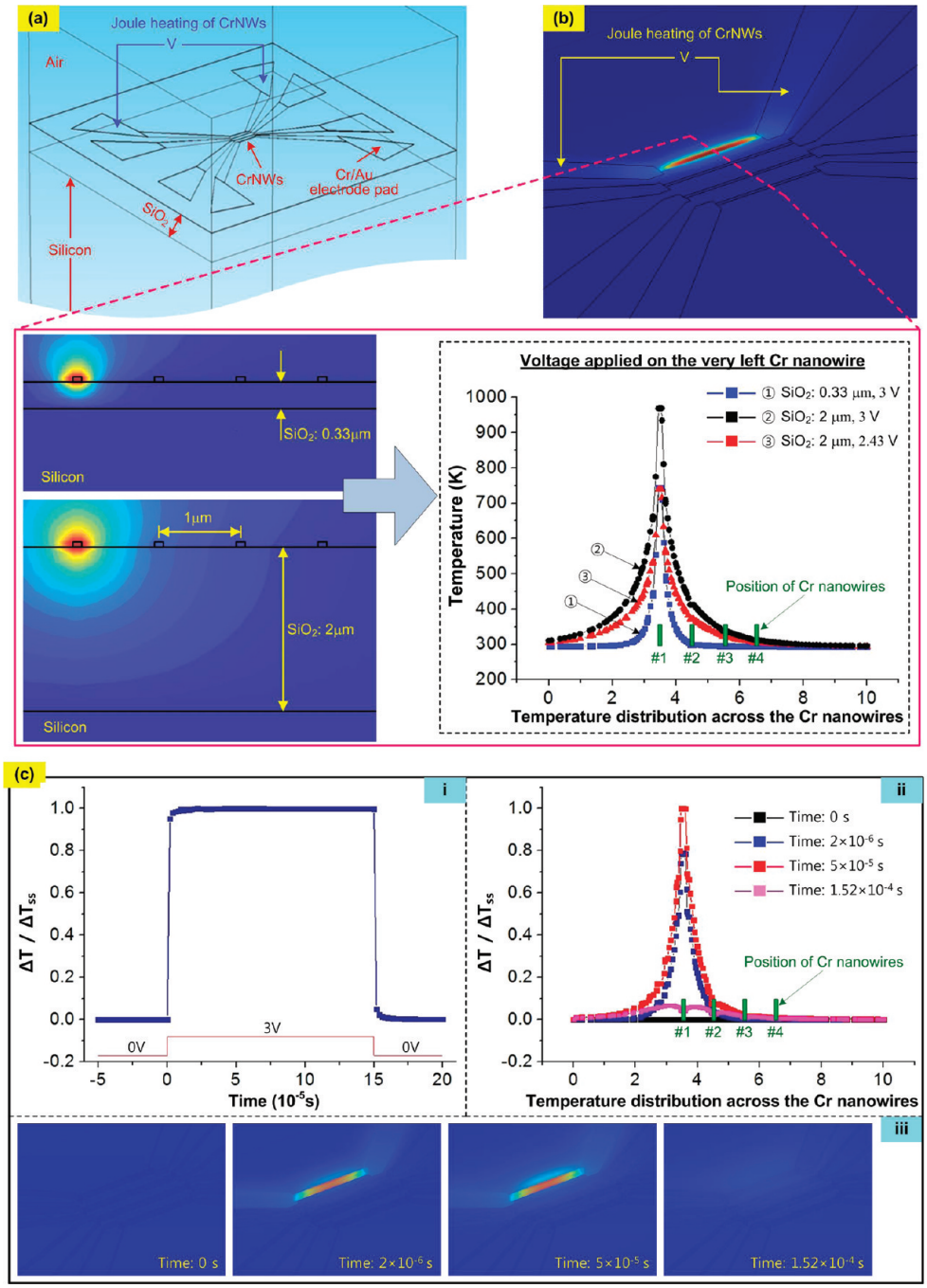

Figure 3. Numerical simulation of nanowire heater array: (a) simulation model; (b) temperature distribution in nanowire array when electrical bias was applied to nanowire #1; and (c) transient thermal analysis when electrical bias was applied to nanowire #1 (i, normalized temperature of center point of nanowire #1; ii and iii, change of normalized temperature distribution in nanowire array along time).

nanowire in the case of t_{SiO_2} = 0.33 μm under an electrical bias of 3 V (Figure 3b①). The local temperature gradient in the lateral direction is 2.2 K/nm at the edge of the heated nanowire. From this high temperature gradient and sharp temperature profile, it can be concluded that the nanowire heater provides a highly localized temperature field with nanoscale resolution. Another notable observation is the thickness effect of the thermal insulation layer (SiO_2). Temperature of the nanowire on a 0.33 μm thick SiO_2 layer (t_{SiO_2} = 0.33 μm, V = 3 V, Figure 3b①) raised (744.4 K) less than that on a 2 μm thick SiO_2 layer (t_{SiO_2} = 2 μm, V = 3 V, Figure 3b②) (969.8 K) under the same electrical bias of 3 V. In order to achieve the same maximum temperature, lower voltage (2.43 V) is required to heat the nanowire on a 2 μm thick SiO_2 layer. However, temperature gradient is higher for t_{SiO_2} = 0.33 μm (2.2 K/nm at the edge of nanowire; ΔT_{NW1}:ΔT_{NW2} = 2.5; $T_{NW1} - T_{NW2}$ = 445.5 K) than for t_{SiO_2} = 2 μm (1.5 K/nm at the edge of nanowire; ΔT_{NW1}:ΔT_{NW2} = 2.0; $T_{NW1} - T_{NW2}$ = 367.8 K) as shown in Figure 3b① and ③. These results are caused by lower thermal conductivity of the SiO_2 layer than those of Si and Cr. A thick SiO_2 layer prevents heat dissipation from the

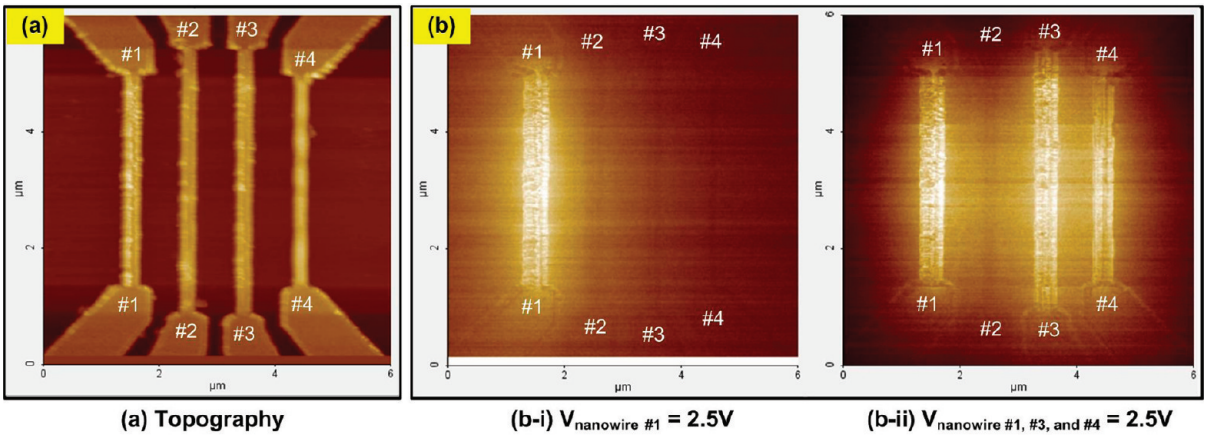

Figure 4. (a) Topography of a Cr nanowire array. (b) Scanning thermal microscopy (SThM) results of local nanoscale heating by individual nanowires (b-1, only nanowire #1 was heated; b-2, nanowires #1, #3, and #4 were heated simultaneously).

nanowires to the Si substrate and facilitates temperature rise of the heated nanowires and their surrounding areas in the lateral direction. On the contrary, a thinner SiO_2 layer drives more vertical heat dissipation toward the Si substrate and thus results in lower maximum temperature of the nanowire heater and less heat dissipation in the lateral direction. In summary, proper thickness of thermal insulation layer should be selected for a compromise between sharper temperature profile and maximum heating temperature. In order to evaluate the heating and cooling speeds of the nanowire heater array, transient thermal analysis was also carried out as shown in Figure 3c. At $t < 0$, no electrical voltage was applied and all the locations including nanowires and surroundings had uniform temperature ($T = 293.15$ K). When an electrical voltage of 3 V was applied at $t = 0\ \mu$s, 95% of steady state temperature ($\Delta T/\Delta T_{ss} = 0.95$; ΔT = temperature increase at time t, ΔT_{ss} = temperature increase at steady state) was achieved only after 2 μs. Also, when electrical voltage was turned off again, only 2 μs of elapse time was required for cooling by 95%. This simulation result reveals that ultrafast local heating and cooling is possible by using the nanowire heater array due to extremely small heat capacity of the nanowire (3.9×10^{-19} J/K).

Localized heating by the nanowire array was experimentally verified by scanning thermal microscopy (SThM). An electrical voltage of 2.5 V was applied in the circuit, and local heating was measured by the output voltage signal from a resistive temperature detector (RTD)-based SThM system (XE-100, Park Systems, Korea). The output voltage is measured across a Wheatstone bridge circuit in which one leg is a platinum (Pt) based SThM probe. When the local surface temperature on the SThM probe is increased, its electrical resistance is linearly increased and the output voltage from the Wheatstone bridge is altered. Therefore, higher output voltage from SThM measurement indicates higher local surface temperature. In Figure 4, local temperature increase was observed in cases of single nanowire heating (nanowire #1) and three nanowire heating (nanowires #1, #3, and #4). For example, $\Delta V = 62$ mV at the center of nanowire #1 vs $\Delta V = 26$ mV at the center of nanowire #2 can be measured in the case of single nanowire heating. Another arbitrary heating profile can be generated in microscale spaces with nanoscale resolution by using multiple nanowire heating as shown in Figure 4b-2. Although accurate measurement of absolute temperatures could not be made due to the complexity and uncertainty of temperature calibration of SThM in nanoscale space, local temperature increase along heated nanowires could be qualitatively verified from the SThM measurement. More precise temperature calibration and quantification will be conducted as a future work by employing a multimode heat transfer model in nanoscale.

The applicability of the nanowire heater array for selective and localized chemical reaction control with nanoscale spatial resolution was experimentally verified first by thermal decomposition and cross-linking of polymer molecules. For the thermal decomposition experiment, ~150 nm thick film of PMMA (poly(methyl methacrylate)) known to thermally decompose at ~523–635 K[19] was spin-coated on the nanowire array device (line width = 110 nm, length = 19 μm (nanowires #1 and #4 from left) and 20 μm (nanowires #2 and #3), thickness = 50 nm, and pitch = 1 μm). Then an electrical bias of 6 V was applied selectively across the nanowire #1 and #4 circuits for Joule heating, and subsequent thermal decomposition reaction of PMMA occurred. According to the numerical analysis, an electrical bias of 6 V heats the nanowires up to 469 K, which is close to the thermal decomposition temperature of PMMA. As shown in Figure 5a, the AFM image at the center of nanowire array clearly indicates that the decomposition of PMMA occurred locally and selectively along the Joule-heated nanowires (#1 and #4). The cross-sectional profile shows nanowire #4 before and after coating with PMMA thin film and after thermal decomposition by Joule heating. From this figure, it can be observed that the top surface profiles of the nanowire before PMMA coating and after PMMA thermal decomposition match well with each other, indicating a complete local ablation of PMMA layer by Joule heating of the nanowire. One application of localized polymer decomposition is a selective surface modification of the nanowires for enhanced selectivity and sensitivity in chemical sensing. In an array of nanowires, individual nanowires can be selectively functionalized with different molecules or nanoparticles by a series of polymer decomposition and functionalization processes. We have demonstrated selective surface modification of a nanowire with zinc oxide (ZnO) nanoparticles. Here, thermally exposed Cr nanowires were selectively modified with ZnO nanoparticles, which were subsequently used as seeds for selective hydrothermal growth of ZnO nanowires, a popular material for versatile applications in optics, optoelectronics, sensors, and actuators.[20−22] First, the PMMA layer was ablated by selective thermal decomposition along the heated nanowires. Then selective surface modification with ZnO nanoparticles was

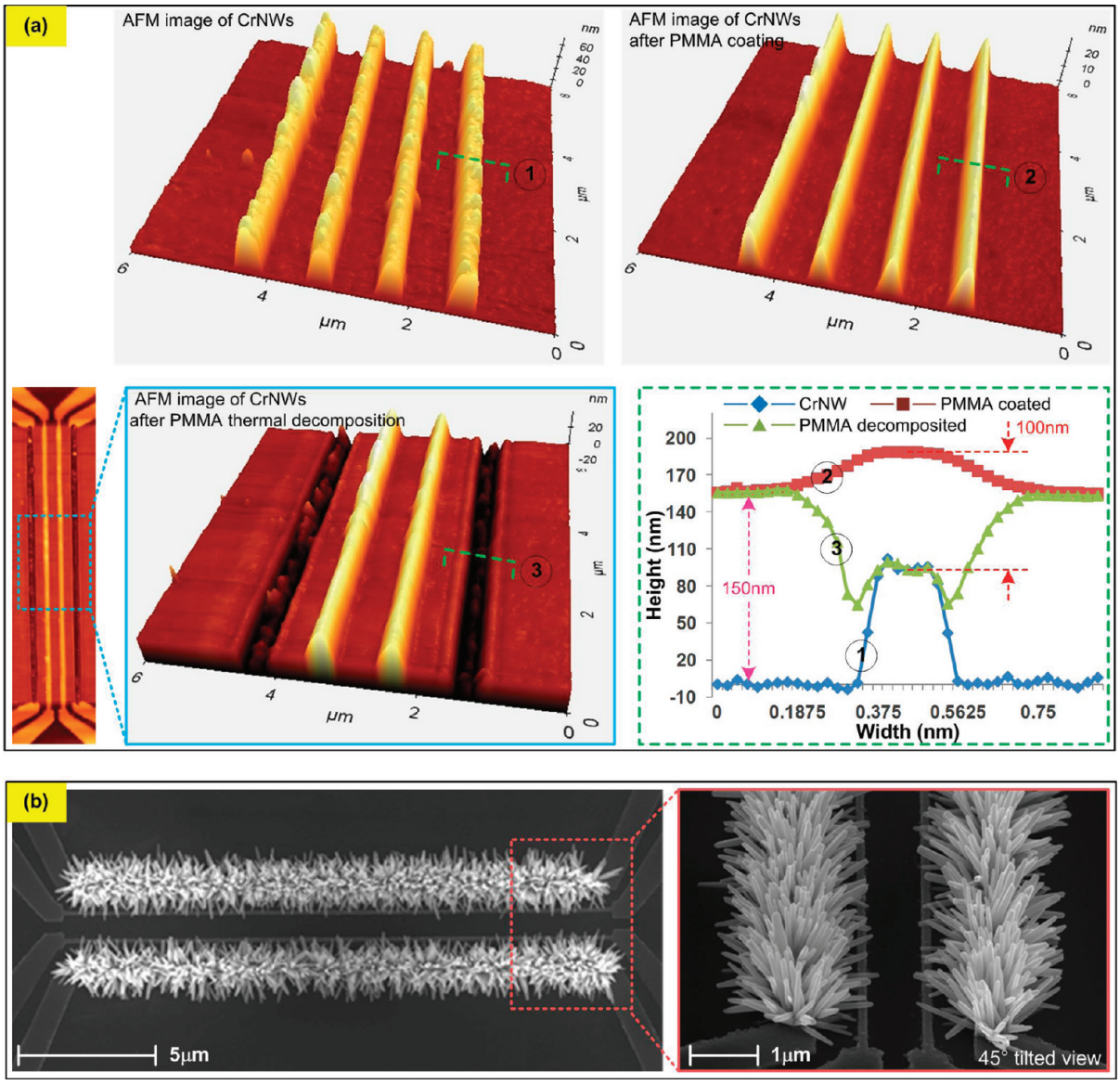

Figure 5. Experimental results of localized thermal decomposition of PMMA, selective surface modification with ZnO nanoparticles, and ZnO nanowire synthesis: (a) AFM images of Cr nanowire array before PMMA coating, after PMMA coating, and after thermal decomposition of PMMA by Joule heating of Cr nanowires #1 and 4 (from left) and cross-sectional profiles of Cr nanowire #4 before and after thermal decomposition of PMMA. (b) SEM image of ZnO nanowires selectively and locally synthesized on the Cr nanowires #1 and 4 (from top) that were exposed by thermal decomposition of PMMA and selectively functionalized by ZnO nanoparticles.

achieved by coating with nanoparticle solution, lift-off, and annealing process.[23] Finally, the chip was submerged in a ZnO precursor solution (zinc nitrate (25 mM), HMTA (25 mM), and PEI (6 mM)) and heated for 45 min at 90 °C for ZnO nanowire synthesis. As Figure 5b shows, ZnO nanowires were selectively synthesized on the Cr nanowires (#1 and #4) that were exposed by thermal decomposition of PMMA via localized Joule heating and subsequently coated with ZnO nanoparticles which served as seeds for the ZnO nanowire synthesis.

In addition to polymer thermal decomposition, the nanowire heaters could also be utilized for selective and localized thermal cross-linking of polymer. On an array of nanowires having the same dimension used for the polymer decomposition experiment, a thin film of azide-terminated polystyrene (PS-*b*-PSN_3) known to thermally cross-link at a temperature of ∼473 K was formed by spin coating. Then electrical bias of 6 V was applied selectively across the nanowires #1 and #4 for Joule heating and thermal cross-linking of the polystyrene molecules. Un-cross-linked polystyrene was removed by dissolving in toluene solvent, whereas cross-linked polystyrene molecules remained on the heated nanowires. As the experimental result in Figure 6 shows, the polystyrene layer around the Joule-heated nanowires was selectively cross-linked and remained, completely covering the nanowires with thicknesses of ∼190 and ∼140 nm on top and side surfaces, respectively. This technique of selective and localized capping of nanowires will be very useful for making reference electrodes that are inert to the surrounding chemical environment in nanowire-array-based chemical sensor applications.

In addition to its usability in a dry air environment, feasibility of the nanowire array heater for localized chemical reaction control

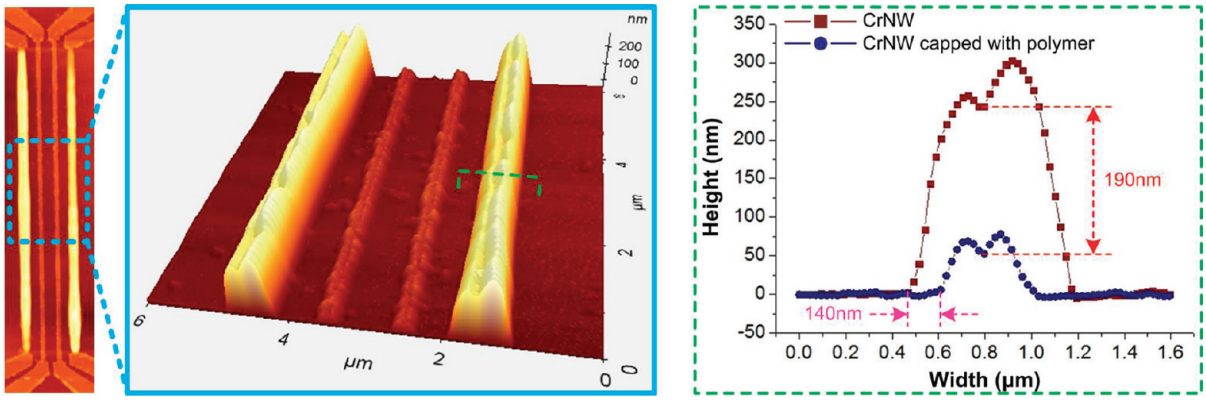

Figure 6. AFM images after localized thermal cross-linking of polystyrene through Joule heating of Cr nanowires #1 and 4 (from left) and cross-sectional profiles of Cr nanowire #4 before and after thermal cross-linking of polystyrene.

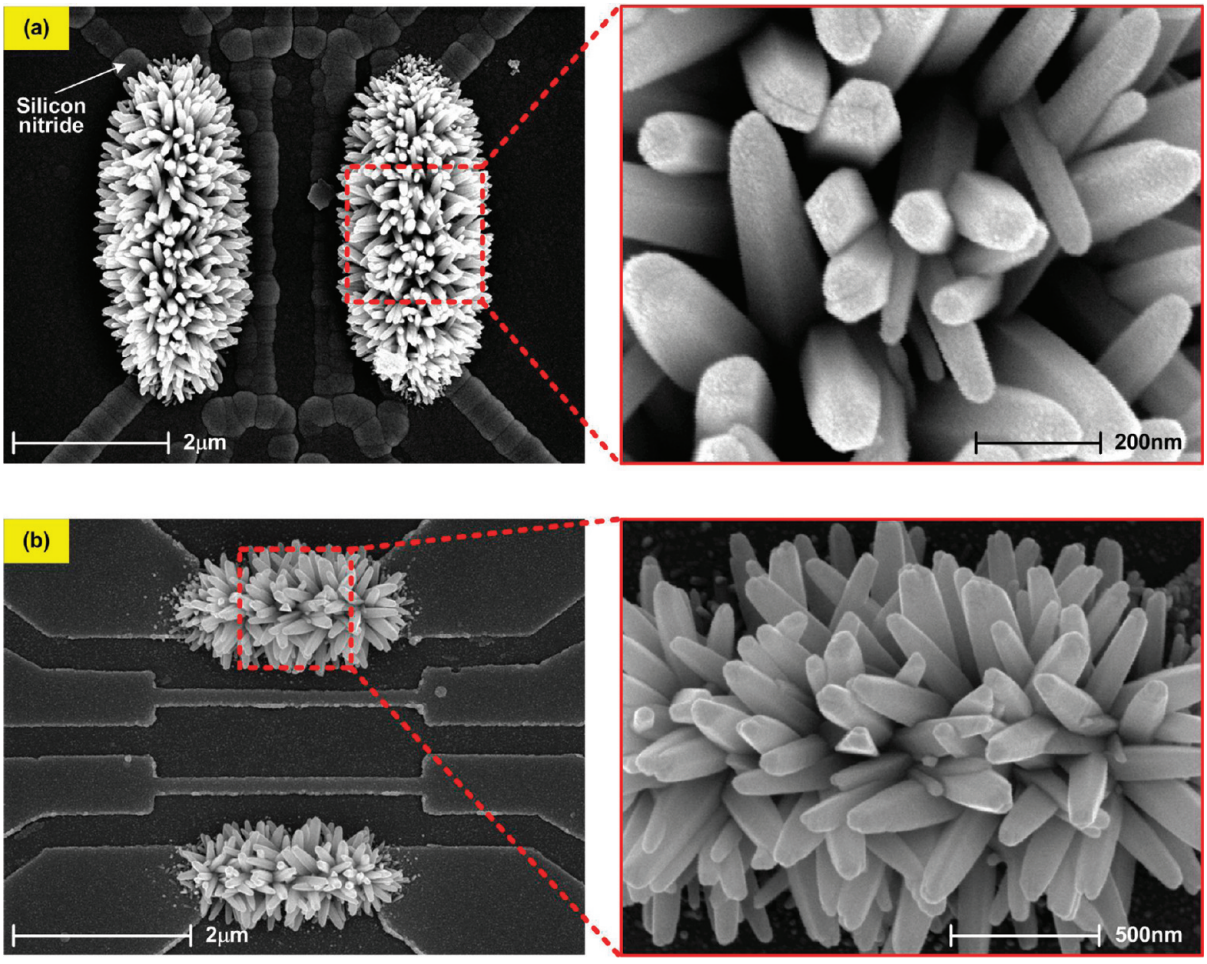

Figure 7. SEM images of locally synthesized ZnO nanowires (a) on a 300 nm thick PECVD silicon nitride film by Joule heating of Cr nanowires #1 and #4 (from left) underneath the silicon nitride film with an electrical bias of 3 V and (b) directly on Cr nanowires #1 and #4 (from top) through Joule heating with electrical bias of 0.8 V and background heating at 353 K by heating plate.

in a liquid environment was verified via temperature-controlled hydrothermal synthesis of ZnO nanowires. The experiment was accomplished by the following three steps: first, a ~300 nm thick silicon nitride film was deposited by plasma enhanced chemical vapor deposition (PECVD) on the nanowire array device. Compared to the dry air environment, a liquid environment requires higher operation voltages to achieve the same heating temperature because of stronger convective heat dissipation through the liquid media. Therefore, it is necessary to protect the metal nanowire electrodes with a passivation layer in order to prevent electrode failure during direct heating of metal nanowires in an aqueous ZnO precursor solution. Second, a ZnO nanoparticle

seed layer was coated by drop-casting on the silicon nitride layer followed by annealing process (at 150 °C on a hot plate for 20 min). Third, a few drops of ZnO precursor solution were applied on the nanowire heater array by using a small PDMS-based liquid container. Finally, an electrical bias of 3 V was applied across the Cr nanowires #1 and #4 to heat up the precursor and induce localized ZnO nanowire synthesis on the heated nanowires. Although the whole surface of the device was coated with ZnO nanoparticle seeds, ZnO nanowires were grown only on the selective area where Joule-heated nanowires (#1 and #4) were underneath, as shown in Figure 7a. This result indicates that the ZnO precursor around the Joule-heated nanowires was locally and selectively heated up to ∼368 K, at which hydrothermal synthesis of ZnO nanowires occurs. In this figure, it is observed that silicon nitride thin film was deposited in a granular conformation around Cr nanowires, which may be due to preferred nucleation around the granular surfaces and rough edges of Cr nanowires. Then ZnO nanowires were selectively grown on the heated Cr nanowires that were passivated with silicon nitride films. The length of ZnO nanowires is maximal at the centers of Cr nanowire heaters, indicating maximum local temperature. On the other hand, a rapid drop of temperature at the side edges of Cr nanowires is observed by short lengths of synthesized ZnO nanowires.

For practical electrical device applications such as sensors, field effect transistors, or energy harvesters, ZnO nanowires have to be electrically connected to the metal electrodes. Therefore direct synthesis of ZnO nanowires on the metal nanowires without any intermediate passiviation layers (e.g., silicon nitride as used above) is necessary. However, as explained above, direct heating of metal nanowires in liquid environment requires a high bias voltage, causing the breakage of metal nanowire. This was circumvented by supplying global background heating of the ZnO precursor solution with a heating plate and applying a lower voltage across the Cr nanowires to achieve the same maximum heating temperature at the local hot spot. By doing this, only ∼0.8 V of electrical voltage was required to generate a temperature of ∼368 K along Cr nanowires under the background heating of ZnO precursor solution at ∼353 K. Even if the precursor solution was heated at ∼353 K, this temperature was not sufficient for the hydrothermal synthesis of ZnO nanowires. On the other hand, the temperature around the Cr nanowire heater was high enough for the fast synthesis of ZnO nanowires. As a result, without any failure of Cr nanowires, ZnO nanowires could be locally and directly synthesized on the Joule-heated Cr nanowires as shown in Figure 7b. Short nanowires with an average diameter of 60 nm and length in the range of 0.5−1 μm were synthesized around the Cr nanowire heaters. This novel method for selective and localized nanowire synthesis provides a much simpler and faster way for the direct integration of nanowires onto functional devices compared to typical random assembly or pick-and-place techniques.[24,25]

In summary, we have developed a novel method for chemical reaction control in a selected nanoscale region via localized temperature control with an array of individually addressable nanowire Joule heaters. Local temperature controllability of the nanowire heater array was verified via numerical simulation and SThM measurement. Then, by several experiments of nanoscale chemical reactions such as thermal decomposition/cross-linking reactions of polymer and hydrothermal synthesis of metal oxide nanowires, we have demonstrated the applicability of nanowire heater array for localized chemical reaction control with nanoscale spatial resolution in both dry and wet environments. It is conceivable that this nanowire-array-based heating device will be very useful for diverse chemical reaction control in nanoscale spaces. Further, due to the extremely small heat capacity of the nanowire heaters, rapid heating/cooling switching capability will find many applications in molecular manipulation such as DNA hybridization/dehybridization. We believe that this novel device will be a very useful tool for nanoscale chemistry control, top-down/bottom-up hybrid nanofabrication, chemical sensing, and biological studies, such as single cell thermal stimulation and molecular manipulation.

AUTHOR INFORMATION

Corresponding Author
*E-mail: inkyu@kaist.ac.kr.

ACKNOWLEDGMENT

This research was supported by the National Research Foundation of Korea (NRF) grant funded by the Ministry of Education, Science and Technology (MEST) (No. 2010-0015290, No. 2011-0004409) and Open Innovation Research Program of Hewlett-Packard (HP) Company. I.P. wants to acknowledge Prof. Bumjoon Kim for the supply of azide-terminated polystyrene (PS-b-PSN3) material and valuable discussions.

REFERENCES

(1) Huber, D. L.; Manginell, R. P.; Samara, M. A.; Kim, B. I.; Bunker, B. C. *Science* **2003**, *301*, 352–354.
(2) Privorotskaya, N.; Liu, Y.-S.; Lee, J.; Zeng, H.; Carlisle, J. A.; Radadia, A.; Millet, L.; Bashir, R.; King, W. P. *Lab Chip* **2010**, *10*, 1135–1141.
(3) Ginet, P.; Montagne, K.; Akiyama, S.; Rajabpour, A.; Taniguchi, A.; Fujii, T.; Sakai, Y.; Kim, B.; Fourmy, D.; Volz, S. *Lab Chip* **2011**, *11*, 1513–1520.
(4) Englander, O; Christensen, D; Kim, J.; Lin, L. *Sens. Actuators, A* **2007**, *135*, 10–15.
(5) Hong, Y. J.; Kim, Y.-J.; Jeon, J.-M.; Kim, M.; Choi, J. H.; Baik, C. W.; Kim, S. I.; Park, S. S.; Kim, J. M.; Yi, G.-C. *Nanotechnology* **2011**, *22*, 205602.
(6) Lapotko, D. O.; Lukianova, E.; Oraevsky, A. A. *Lasers Surg. Med.* **2006**, *38*, 631–642.
(7) Hamann, H. F.; O'boyle, M.; Martin, Y. C.; Rooks, M.; Wickramasinghe, H. K. *Nat. Mater.* **2006**, *5*, 383–387.
(8) Kuwahara, M.; Li, J.; Mihalcea, C.; Atoda, N.; Tominaga, J.; Shi, L. P. *Jpn. J. Appl. Phys.* **2002**, *41*, L1022–L1024.
(9) Shinagawa, T.; Abe, Y.; Matsumoto, H.; Li, B.; Murakami, K.; Okada, N.; Tadatomo, K.; Kannaka, M.; Fujii, H. *Phys. Status Solidi C* **2010**, *7*, 2165–2167.
(10) Lee, S.-H.; Jung, Y.; Agarwal, R. *Nat. Nanotechnol.* **2007**, *2*, 626–630.
(11) Xiong, F.; Liao, A.; Pop, E. *Appl. Phys. Lett.* **2009**, *95*, 243103.
(12) Ward, D. R.; Halas, N. J.; Natelson, D. *Appl. Phys. Lett.* **2008**, *93*, 213108.
(13) Offermans, P.; Tong, H. D.; van Rijn, C. J. M.; Merken, P.; Brongersma, S. H.; Crego-Calama, M. *Appl. Phys. Lett.* **2009**, *94*, 223110.
(14) Yang, F.; Taggart, D. K.; Penner, R. M. *Small* **2010**, *6*, 1422–1429.
(15) Park, I.; Li, Z.; Li, X.; Pisano, A. P.; Williams, R. S. *Biosens. Biolelectron.* **2007**, *22*, 2065–2070.
(16) Park, I.; Li, Z.; Pisano, A. P.; Williams, R. S. *Nanotechnology* **2010**, *21*, 015501.
(17) Park, I.; Li, Z.; Pisano, A. P.; Williams, R. S. *Nano Lett.* **2007**, *7*, 3106–3111.

(18) Park, I.; Ko, S.-H.; Li, Z.; Pisano, A. P.; Grigoropoulos, C. P. *Transducers 2009*; IEEE: Piscataway, NJ, 2009
(19) Manring, L. E. *Macromolecules* **1991**, *24*, 3304–3309.
(20) Bao, J.; Zimmler, M. A.; Capasso, F. *Nano Lett.* **2006**, *6*, 1719–1722.
(21) Tseng, Y.-K.; Huang, C.-J.; Cheng, H.-M.; Lin, I.-N.; Liu, K.-S.; Chen, I.-C. *Adv. Funct. Mater.* **2003**, *13*, 811–814.
(22) Wang, Z. L.; Song, J. *Science* **2006**, *312*, 242–246.
(23) Lim, M. A.; Lee, Y. W.; Han, S. W.; Park, I. *Nanotechnology* **2011**, *22*, 035601.
(24) Mølhave, K.; Hansen, T. M.; Madsen, D. N.; Bøggild, P. *J. Nanosci. Nanotechnol.* **2004**, *4*, 279–282.
(25) Freer, E. M.; Grachev, O.; Stumbo, D. P. *Nat. Nanotechnol.* **2010**, *5*, 525–530.
(26) Xiong, F.; Liao, A. D.; Estrada, D.; Pop, E. *Science* **2011**, *332*, 568–570.

■ NOTE ADDED AFTER ASAP PUBLICATION

This article was published ASAP on October 7, 2011. Reference 26 has been added. The corrected version was posted on October 20, 2011.